Acoustic emission studies on fracture behaviour of CFC-materials under various loads.

Patrick, Majerus, Forschungszentrum Jülich EURATOM-Association, Jülich, Germany;
Jeremie, Compan, Université Pierre et Marie Curie, Paris, France;
Takeshi, Hirai, Forschungszentrum Jülich EURATOM-Association, Jülich, Germany;
Jochen, Linke, Forschungszentrum Jülich EURATOM-Association, Jülich, Germany;
Reinhard May, Fraunhofer Institut Zerstörungsfreie Prüfung, Dresden, Germany;

Abstract

Carbon fiber composites (CFCs) are promising Plasma-Facing-Material (PFM) candidates for the area exposed to high heat loads in future fusion devices. However recent studies show that CFCs suffer from erosion due to brittle destruction under thermal loads. The mechanism of brittle destruction of CFCs and the interactions between matrix and fibres under loading have not been fully understood yet. In order to study these mechanisms, acoustic emission (AE) technique shall be applied. As a first step fundamental studies on CFC were performed under various loads. Calibration experiments on reference materials, such as different metals and graphite were made with the goal to compare the propagation of sound with the acoustic properties, attenuation and sound speed in CFCs. Further micro indentation testing revealed a correlation between mechanically dissipated energy and pseudo energy recorded by AE. A time frequency analysis has been developed to additionally study these AE-signals. During tensile tests, the stress strain behaviour of the CFC-material was divided into a linear-elastic and quasi-plastic part, whereas the quasi-plastic part was accompanied by massive AE-events. The evolution of failure could be studied by localising events at different load steps. Young's moduli for two of the three orthogonal orientations determined by the tensile tests and by the sound velocity were in agreement.

1 Introduction

One of the most attractive alternatives to common energy sources represents nuclear fusion as it is not producing any atmospheric pollution and it is further virtually inexhaustible. Along with this very attractive goal, nuclear fusion is an unprecedented scientific and technological challenge. In order to demonstrate the physical and technological feasibility of a controlled thermonuclear reaction, the joint project of the International Thermonuclear Experimental Reactor (ITER) has been initiated. The design of ITER relies on a solid and robust basis of experimental results and sophisticated modelling. However, there are still a number of issues for which the existing database is still fragmentary or which are critical on the basis of extrapolation from present fusion devices [1].

Presently carbon fibre composite materials (CFC) are planned to be used for the high heat flux regions of the divertor [2]. Due to their excellent thermal conductivity, favourable mechanical properties, and a good plasma compatibility, CFCs have been used successfully in most of the present day tokamak and stellerator experiments worldwide. In particular high heat flux components with CFC armour have demonstrated their superior thermal shock behaviour under cyclic and off-normal transient heat loads without competition. Transient thermal loads can deposit energy densities of several ten MJ/m² with pulse durations in the order of a few milliseconds and erode the plasma facing material. In carbon based materials the erosion process is dominated by brittle destruction, a process which is associated with the formation of carbon dust by emitting particles from the eroded surface [3]. Up to now only limited information is available on erosion mechanisms under these events.

In order close this leak of knowledge, high heat flux experiments have been performed in electron beam test facilities [4, 5]. Extensive diagnostics such as beam current and calorimetric measurements together with sophisticated in-situ studies of the released particles led to an enhanced understanding of the phenomenon [6,7]. Especially in-situ optical diagnostics represent a very unique experimental tool; first data obtained with these methods have great impact on the modelling of the dynamic erosion processes [8]. To further extend the applied diagnostics it is planned to use acoustic emission techniques. Especially the onset of brittle destruction, the discrimination between fibre and matrix erosion, and the energy release rate of the emitted particles shall be addressed by this undertaking.

AE has proven to offer the potential to detect the evolution of damage as it appears in ceramic matrix composites. Among a number of distinct advantages, one is the possibility to calculate the spatial source location based on arrival time differences between a number of sensors [9]. However, only limited work has been undertaken to understand the acoustic emission signals that are generated by ceramic-matrix composites under different loading. Most available publications deal with the time domain, i.e. the number of acoustic events as a function of time (or load) in order to detect the onset of matrix or fibre cracking [10,11]. Nethertheless some authors have successfully monitored the accumulation of damage during tensile tests as well as correlating the individual AE signals in terms of waveform analysis [12, 13] or in terms of parametric studies like duration and energy [10] to specific damage events such as matrix cracking, interface debonding and delamination cracking.

The goal of the present paper is to perform basic AE studies on CFCs in order to demarcate the possible applications in the frame of brittle destruction investigations under electron beam thermal loads. As a first step attenuation and velocity of sound waves in the involved materials are addressed. By performing indentation tests it is further expected to draw a correlation between mechanically dissipated energy and pseudo energy recorded by AE. As indents can be placed either in fibre or matrix it is believed to find also differences in the characteristics of the waves. One method to analyse AE signals is the Fast-Fourier Transform (FFT). As in classical FFT either time or frequency can be obtained, a windowed time frequency analysis has been adopted. The potential to detect the onset failure, such as matrix cracking, shall finally be verified by tensile tests in all three orthogonal orientations.

2 Materials

Both NB31 and NS31 are advanced, high thermal conductivity CFCs manufactured by the SNECMA group. They are constituted by a NOVOLTEX preform with P55 ex-pitch fibres in the x-orientation and ex-PAN fibres in the y-orientation; these CFCs undergo a subsequent needling which gives an reinforcement in the z-orientation. The volumetric fraction of fibres are 35% (27% in x-, 5% in y- and 2% in z-orientation). The high thermal conductivity orientation is that of P55 ex-pitch fibres (x-orientation). The densification is performed by chemical infiltration of pyrocarbon at 1000°C, followed by a graphitisation heat treatment at 2800°C. The last phase of densification is made by chemical infiltration at 1000 °C and a pitch impregnation at 100 MPa and 1000°C [14]. NS31 is produced by final infiltration of liquid silicon leading partly to the formation of silicon carbide. NS31 contains about 8–10 at.% of silicon, its porosity is about 3–5% and its density is about 2.1 g/cm³ [15]. The un-doped NB31 has an average density of 1.91 g/cm³. As reference materials, stainless steel, structural steel, CuZrCr (Cu-alloy) and the fine grained graphite (V1325) from Ringsdorffwerke has been used for the present study. This graphite exhibits a density of 1.89 g/cm³ and has an open porosity of 5.3 %.

3 Experimental equipment and analysing methods

Acoustic emission

AE was monitored with a AMSY4 system from Vallen with three individual channels. Two different types of sensors have been used: Wide band (300 – 2000 kHz) Vallen sensors (VS2M-P), with resonances at 320, respectively 790 kHz (addressed as sensor P); a symmetric sensor (sensor S) with an BNO connector and integrating cable (Type KAR 601 S), having a flat response between 100 and 600 kHz. The acquisition system is relatively efficient in the fact that it digitises the true, multiple frequency waveform (TR-mode) and additionally calculates certain parameters of the waveform. The system consisted of a built in Pentium PC with a 32bit, 10 MHz acquisition. The preamplifier gain was set at 34dB. In order to localise the sources of AE signals, a standard localisation technique depending on run-time differences of AE signals collected by both acoustic sensors, has been applied [16].

Indentation

The instrumented depth-sensing micro-indenter provides a highly precise information of the indenter position at a given applied load. FISHERSCOPE H100, the instrument used in the present study, records the displacement of the in-built Vicker's indenter with an accuracy in the nanometer range and a load resolution of 0.4 mN up to 1000 mN. The principles of determining Young's modulus, hardness and dissipated energy from a micro-indentation test has been illustrated elsewhere [17]. To apply higher loads a second Vicker's indenter set-up, the micro hardness tester MICROMET 1 from Buehler LTD was utilised. Here it was possible to achieve loads between one and 100 N. However, the possibility to calculate dissipated energy was not given. The goal of testing was to monitor signals of higher amplitude for an enhanced time frequency analysis.

Tensile tests

Tensile tests were conducted at room temperature on an INSTRON 5565 facility. Flat dogbone specimens with a length of 65 mm, a maximum width of 20 mm (8 mm, resp. 6 mm within the measurement length) and a thickness of 5 mm were used for x- and y-orientational testing. The z-type samples consisted of a cylindrical design with 30 mm in length and 20 mm maximum diameter (Figure 4 - Figure 6). The specimens were cut from blocks by using a CNC machine equipped with diamond-coated fingermills. The specimens were fixed by Instron clamps (Cat 2716-010) allowing loads up to 5 kN. A standard Instron load cell (2518-103 Series) with a dynamic range of 5 kN and an extensometer (CAT NO 2620-603) with a 1 mm gauge length were used to measure the stress-strain parameters. All the tests were conducted strain controlled (0.5 %/min) in accordance to the European Standard (EN 658-1).

AE waveform analysis

AE waveform contains information of fracture frequency emitted from materials. To analyse the frequency of AE waveform, Fourier transform and Fast Fourier Transform (FFT) are widely used [18, 19, 20]. The definition of Fourier transformation is written as follows:

$$X(f) = \int_0^{\infty} x(t) \cdot \exp(-i2\pi ft)dt \qquad (1)$$

The signals acquired in experiments are sets of discrete data points. In this case, FFT analysis can be applied. It is written by the following equation:

$$C_k = \frac{T}{N}\sum_{j=0}^{N-1} x(j) \cdot \exp\left[-i2\pi \frac{jk}{N}\right] \qquad (k = 0,1,2,\ldots,N/2) \qquad (2)$$

where C_k, T, N, x_j and k are the amplitude in frequency domain, acquisition time, the number of sampling data points, the j-th data point and scaling corresponding to frequency, respectively. In the present study, windowed FFT was used in order to analyse time evolution of frequency bands. In this analysis, the data in a time-window were cut and analysed by FFT. Time evolution is obtained by shifting the time-window, i.e. shifting the analysing period, step by step. The shape of the time-window is rectangular with cosine curve edges to reduce artificial effects of the sharp edge at the time-window boundaries. The time resolution and the band width of windowed FFT depend on the size of the time window. The minimum frequency is about 20 kHz at a time resolution of about 50 µs and the maximum frequency was 600 kHz limited by the piezoelectric sensor. The signals were recorded with a time resolution of 5 MHz.

4 Results

Sound velocity and signal attenuation

AE was used to measure the sound velocity. This was accomplished by using one sensor (P) as transmitter of a predefined signal. The amplitude of the emitted signal has been measured to be 87,8 dB (24,5 mV) by directly coupling sensor P to the receiving sensor (S). From the distance L between the AE sensors, and the difference in times Δt of arrival of the first peak, the experimentally determined velocity of the extensional wave C_e, was calculated. The extensional waveform component for which the particle motion is in the plane of the plate and in the direction of the propagation travels at a higher velocity and exhibits little or no dispersion, meaning that all frequency components travel at approximately the same velocity [9].

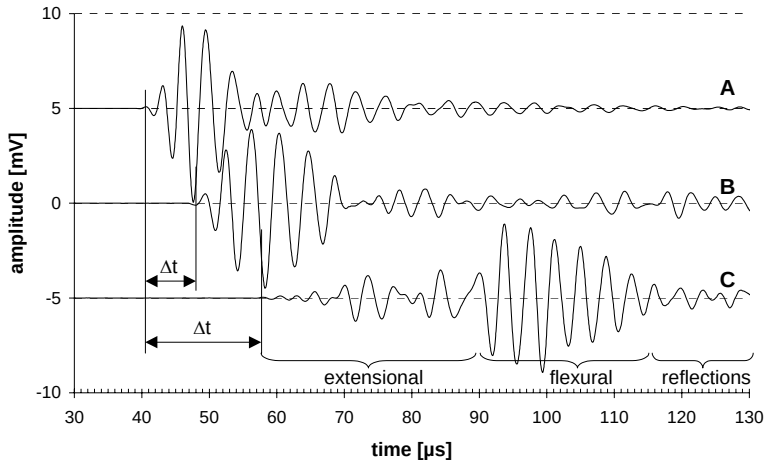

Figure 1: Acoustic waveforms to measure speed of sound. A: Sound wave from the transmitted signal; registered by directly coupling sensor P to the receiving sensor (reduced in amplitude by factor 5). B: Received signal from a 65 mm long CFC-specimen (ex-pitch orientation). C: Received signal from a 135 mm long stainless steel cylinder.

Figure 1 shows the principle approach to determine Δt. However, a clear differentiation between extensional and flexural wave only became possible for the different metals used as reference materials. Therefore the first burst of the received signal was used to calculate the sound velocity of the carbon based materials and composites.

From classical plate theory where the wavelength is much larger than the plate thickness and the direction of wave propagation is in the main symmetry direction of an orthotropic

laminated plate, the velocity of an extensional wave, c_e, is related to the longitudinal elastic modulus, E, in the following form, where ρ is the density of the material [12]:

$$c_e = \sqrt{\frac{E}{\rho}} \tag{3}$$

These measurements were performed on the tensile test samples before testing and on the CFC-blocks before manufacturing the samples. The results of the measurements are summarised in Table 1. For each value a minimum of 4 and a maximum of 8 measurements were averaged. The standard deviation of the measured results is shown in italics. No significant difference was revealed between blocks and thin tensile samples. Thus it was concluded that the influence of sample thickness was negligible and plate theory to calculate Young's modulus could be applied. The distance $L_{50\%}$ for a signal amplitude attenuation of 50% was calculated by the following equation:

$$L_{50\%} = \frac{\ln(0.5)}{A} \qquad \text{with} \qquad A = \frac{1}{L} \cdot \ln\left(\frac{a_{emitted}}{a_{received}}\right) \tag{4}$$

where A is attenuation, $a_{emitted}$ and $a_{received}$ are the amplitudes of the emitted and received signals, respectively over the distance L between the two sensors.

	Graphite	CFC NB31			CFC NS31		
	V1325	ex-pitch	ex-PAN	needling	ex-pitch	ex-PAN	needling
sound velocity	2785	8950	1670	1670	9800	2465	2287
[m/s]	*53*	*195*	*170*	*37*	*480*	*152*	*38*
attenuation [1/m]	-52.4	-32.4	-134	-125	-55.9	-59.2	-73.3
Distance for 50%	13.8	22.5	5.9	5.6	12.6	11.7	9.5
attenuation [mm]	*2.4*	*3.9*	*1.9*	*0.6*	*1.8*	*0.5*	*0.6*
E [GPa]	14.7	152	5.3	5.3	203	12.8	11.2
by AE	*0.6*	*6.7*	*1.1*	*0.24*	*20*	*1.6*	*0.37*
E [GPa]		139	19.4	5.6		21	10.1
by tensile testing		*12.6*	*1.7*	*0.45*		*1.9*	*0.73*

Table 1: Sound velocity and attenuation in dependency of material and orthogonal orientation. Young's modulus determined by AE compared to results from tensile testing. The numbers in italics represent the standard deviations (±) from the testing series.

The standard deviation is an indication of the reliability of the measurements. A good reproducibility was given for the sound velocity in graphite and in needling direction of the CFCs. The rather high velocities in the ex-pitch fibre orientation in combination with the limited sample length (65 mm for NB31; 20 mm for NS31) demand a more precise determination of Δt as it is possible with the present equipment. The ex-PAN orientation exhibited a relatively high scattering of data. Also the Young's Modulus determined by AE did not correspond with the values from mechanical testing as it was the case for the other two directions. In NB31 attenuation of the signal was weaker in the ex-pitch orientation while the orientation does not seem to influence attenuation in the Si-doped CFC.

Indentation testing

Indentations were placed into the fibres and between the fibres (matrix) at loads of 500, 800 and 1000 mN, respectively. Loading time was 2 s. AE threshold (sensor S) was set to 25,1 dB. As for the pure graphite and for the matrix no AE-signals were detected, the study

was concentrated on the carbon-fibres. Indentation analyses tend to result in important scattering of the obtained values. Therefor it is essential to use statistics in order to interpret the results. In the present study, each time the values from 7 indentations per applied load were averaged. To conclude on the acoustic energy at the location of the indentation the attenuation over the distance between sensor and indentation spot was considered. The calculations were based on the attenuation values given in Table 1. To do so it was stated that attenuation of amplitude and of energy have a similar characteristics. This statement was consolidated by the fact, that accumulation of amplitude and of energy over time during one indentation were comparable. The correlation of mechanically dissipated energy and pseudo energy measured by AE is shown in Figure 2. An almost linear correlation between the two energies becomes obvious with almost no influence of the kind of fibres. The fact that higher energies at the same loads are dissipated in NS31 compared to NB31 allowed to cover a higher range of values. Although the measurements are accompanied by significant scattering it seems to be possible to calibrate the pseudo energy of the AE signals via indentation tests.

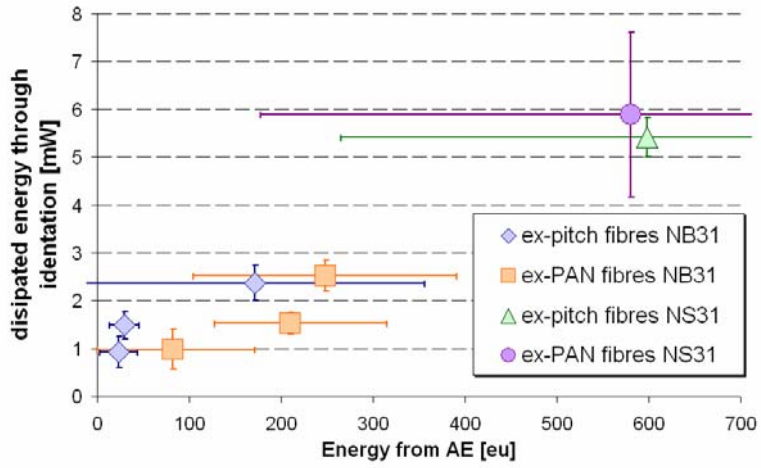

Figure 2: Correlation between mechanically dissipated energy and pseudo energy measured by AE. The error bars show the standard deviations.

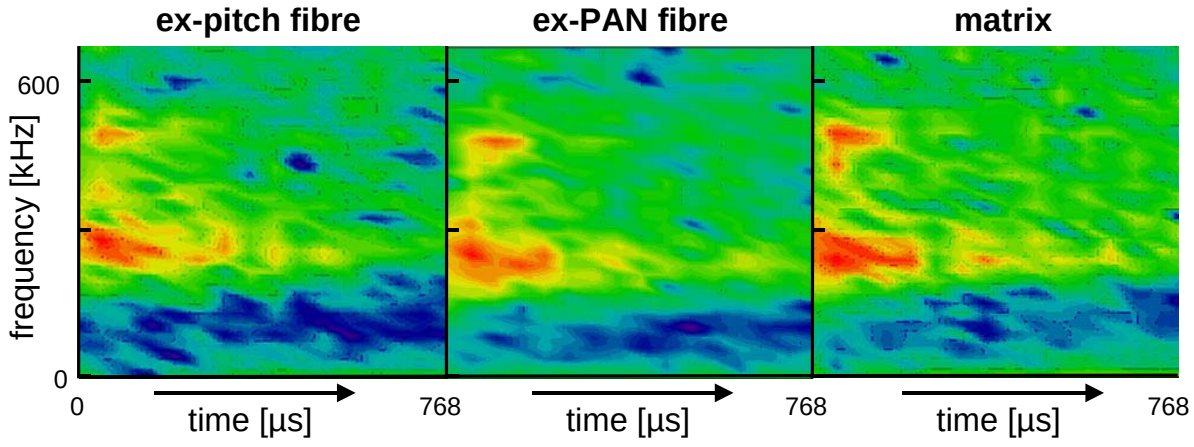

Figure 3: Normalised AE Signals obtained at the micro hardness tester at loads of 100 N analysed by windowed FFT (NB31). Small (blue) to high (red) amplitudes.

AE signals obtained from micro hardness tests at loads of 100 N were compared by windowed FFT. Here also indents into the matrix produced AE-signals, unlike to the graphite. Figure 3 shows amplitude-normalised AE Signals by windowed FFT obtained for matrix, ex-pitch and ex-PAN fibres. Unfortunately no differences in the frequency time domain could be observed up to the present state of the study.

Tensile tests

In the present investigations the AE sensors could, as a difference to other studies [10, 11, 12], not be connected directly to the tensile test samples as they were too short. Therefor it became necessary to use sound guiding wires. These 1,5 mm thick wires were connected in each case directly to the heads of the specimen. As the thin sound wires modulate the signal frequency FFT analyse became needless. Thus only the P-sensors with a resonance response, leading to a higher sensibility were used. Threshold values between 40 and 52 dB were applied. Within this range no influence was found on the strain related starting point. With lower strain rates, an overloading of the acquisition occurred. Load and strain were recorded via 10 V signals provided by the load frame. Up to 8 tests per orientation were conducted. Here only one example per direction is shown for NB31. The average value of the starting slope (Young's modulus) is given in Table 1.

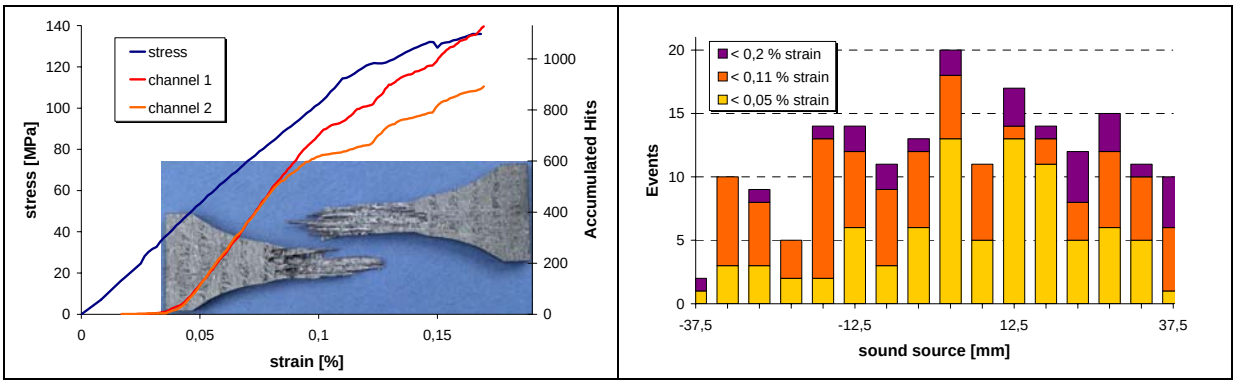

Figure 4: Tensile testing in ex-pitch (X) orientation. Left side: Stress and accumulated hits over strain + specimen after testing. Right side: Number of events over location for three different strain ranges.

Figure 4 - Figure 6 show the stress strain behaviour and AE-hit accumulation over the strain. The non-linear response, differently pronounced for the three orientations, is mostly the result of transverse matrix cracks, although, additional damage mechanisms such as interlaminar matrix cracks and fiber breaks may also contribute to this behaviour. This results in matrix cracks that are bridged by unbroken fibres. In the vicinity of the matrix cracks, the bridging fibers experience higher strains than fibers in areas without matrix cracks, which is the cause of non-linearity. It should be noted that the first damage events occurred at stress levels prior to the initiation of non-linear behaviour. This is also in a good agreement with previous studies [12].

The figures additionally show the broken samples after testing (picture) and the amount of events for three different strains, as a function one directional location (0 mm represent the centre of the samples). To calculate the location of the events, the orientation dependant sound velocity (Table 1) was applied. Due to the relatively high threshold and the strong signal attenuation the location of the events was not very precise. In other words, if a signal was emitted at one end of the sample, the sensor close to this event might catch the first burst while the signal at the second sensor might only reach the threshold value at a higher amplitude wave later in the signal. However a general tendency of the signal origin could be given. In the ex-pitch orientation the events were widely distributed over the whole specimen length during the whole testing. At the end of the test also fracture appeared to be largely spread over the sample length. In ex-PAN orientation, from the beginning of registering events, a clear tendency indicated an area of higher activity, confirmed by the fracture within this area. In the Z-orientation, the emitted events were first homogeneously distributed over the sample length. This suggests an homogeneous distribution of the strain. Only close to

fracture at strains above 0.2 %, it came to a localisation of the AE events in the area of final failure.

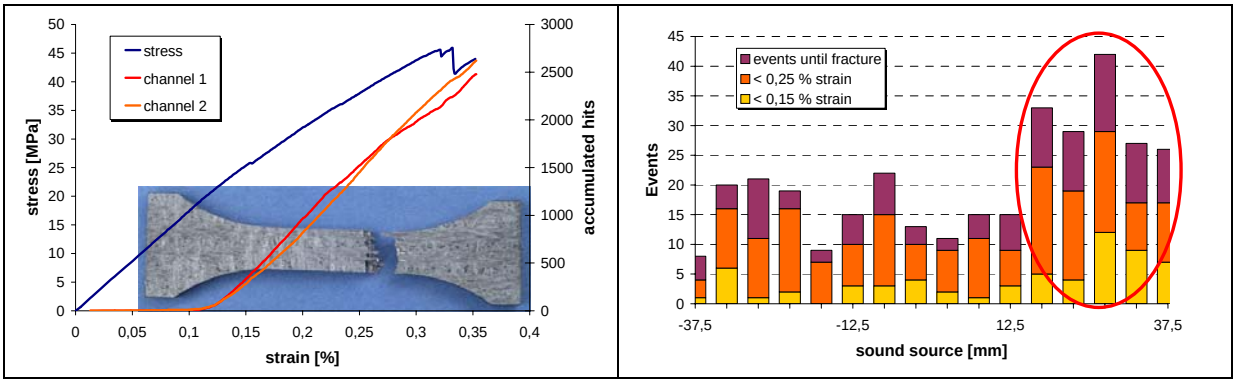

Figure 5: Tensile testing in ex-PAN (Y) orientation.

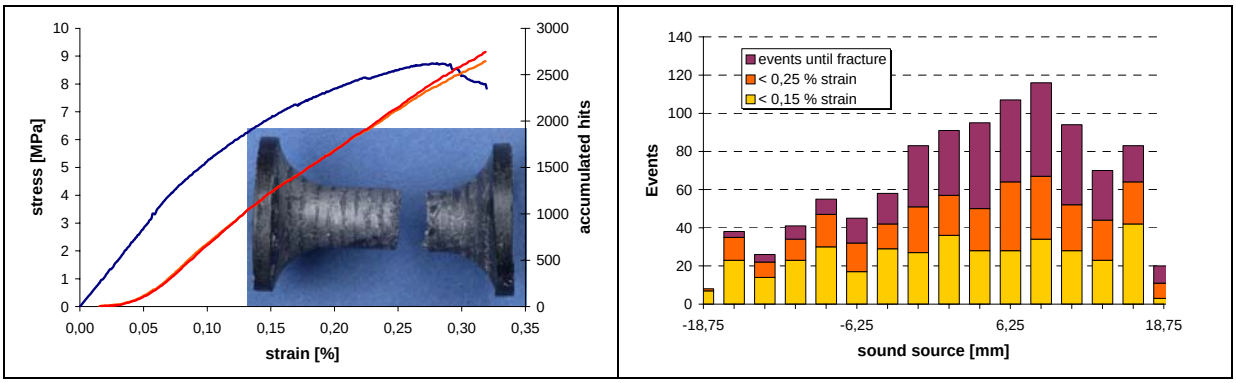

Figure 6: Tensile testing in needling (Z) orientation.

5 Conclusion

The goal of the present study was to demarcate the possible applications of AE in the frame of brittle destruction investigations. Especially the onset of brittle destruction, the discrimination between fibre and matrix erosion, and the energy release rate of the emitted particles should be addressed. From the results obtained by tensile testing it becomes clear that AE is a powerful tool to detect the onset of cracking within composite materials earlier than by other methods. This has also been shown in other applications [16] and is thus seen to be rather promising in detecting the onset of brittle destruction under high transient heat loads. The indentation tests further revealed a correlation between mechanically dissipated energy and pseudo energy, recorded by AE. This gives rise to the assumption that an acquisition of energy release by means of AE during brittle destruction could be possible. The frequencies of AE signals were almost unchanged for indentations at different locations of the CFC materials which confirms previous results obtained by other authors [13]. However flexural mode and shear mode of the sound waves in terms of frequency dependant sound velocities have still not been considered in the present study. Thus it is believed that further investigation of the potential of this type of analysis will lead to more intelligent and quantitative AE results and thus to an enhanced application range.

References

[1] R. Andreani, M. Gasparotto, "Overview of fusion nuclear technology in Europe", Fusion Engineering and Design 61-62 (2002) 27-36

[2] W. Daenner, M. Merola, P. Lorenzetto, A. Peacock, I. Bobin-Vastra, L. Briottet, B. Bucci, D. Conchon, A. Erskine, F. Escourbiac, M. Febvre, M. Grattarola, C.G. Hjorth, G. Hofmann, A. Ilzhoefer, K. Lill, A. Lind, J. Linke, W. Richards, E. Rigal, M. Roedig, F. Saint-Antonin, B. Schedler, J. Schlosser, S. Tahtinen, E. Visca, "Status of fabrication development for plasma facing components in the EU", Fusion Engineering and Design 61-62 (2002) 61-70

[3] J. Linke, M. Akiba, R. Duwe, A. Lodato, H.-J. Penkalla, M. Rödig, K. Schöpflin, "Material degradation and particle formation under transient thermal loads", Journal of Nuclear Materials 290-293 (2001) 1102-1006

[4] J. Linke, H. Bolt, P. Chappuis, H.-J. Penkalla, M. Scheerer, K. Schöpflin, "Brittle destruction of carbon based materials under severe thermal loads", Fusion Engineering and Design 49-50 (2000) 235-242

[5] J. Linke, S. Amouroux, E. Berthe, Y. Koza, W. Kühnlein, M. Rödig, "Brittle destruction of carbon-based materials in transient heat load tests", Fusion Engineering and Design 66-68 (2003) 395-399

[6] T. Hirai, J. Linke, W. Kuehnlein, G. Sergienko, S. Brezinsek, Light emisson from carbon based materials under ITER relevant thermal shock loads, Journal of Nuclear Materials 321 (2003) 110-114.

[7] T. Hirai, S. Brezinsek, W. Kuehnlein, J. Linke, M. Roedig, G. Sergienko, "Particle release from carbon based materials under intense transient heat loads", 10th Int. workshop on carbon materials for fusion application, to be published

[8] S. Pestchanyi, H. Wuerz, "3-D simulation of macroscopic erosion of CFC under ITER off-normal heat loads", Fusion Engineering and Design 66-68 (2003) 271-276

[9] M. Surgeon, M. Wevers, "One sensor linear location of acoustic emission events using plate wave theories.", Materials Science and Engineering A265 (1999) 254-261

[10] M. Laux, H. Klauß, L. Haupt, B. Köhler, E. Chilla, C. Flannery, "Mechanical and sound investigations of advanced carbon materials" Proceedings of the 10th Carbon Workshop, Juelich, Germany, 2003

[11] M. Surgeon, E. Vanswijgenhoven, M. Wevers, O. Van Der Biest, "Acoustic emission during tensile testing of SiC-fibre-reinforced BMAS glass-ceramic composites", Composites Part A 28A (1997) 473-480.

[12] G.M. Morscher, A.L. Geyekenyesi, "The velocity and attenuation of acoustic emission waves in SiC/SiC Composites", Composites Science and Technology 62 (2002) 1171-1180

[13] Q-Q. Ni, M. Iwamoto, "Wavelet transform of acoustic emission signals in failure of model composites", Engineering Fracture Mechanics 69 (2002) 717-728.

[14] T.D. Marshall, R.J. Pawelko, R.A. Anderl, G.R. Smolik, B.J. Merrill, R.L. Moore, D.A. Petti, "Oxygen reactivity of a carbon fibre composite", Fusion Engineering and Design 69 (2003) 663-667

[15] J.P. Bonal, C.H. Wu, D. Gosset, "Simulation experimental investigation of plasma off-normal events on advanced silicon doped CFC-NS31", Journal of Nuclear Materials 307-311 (2002) 100-105

[16] R. Herzog, P. Majerus, J. Mönch, R.W. Steinbrech, F. Schubert, L. Singheiser, "Study of crack development in APS and EB-PVD TBCs with bending tests using acoustic emission and in-situ visual observation", Proceedings of the 27th Annual International Conference on Advanced Ceramics & Composites, January 26-31, 2003, Cocoa Beach, Florida

[17] P.A. Sundaram, D. Basu, R.W. Steinbrech, P.J. Ennis, W.J. Quadakkers, L. Singheiser, "Effect of hydrogen on the elastic modulus and hardness of gamma titanium aluminides", Scripta Materialia, Vol. 41, No. 8, pp. 839-845, 1999

[18] M. Laux, H. Pursch, “Sound emission from an arc cathode”, IEEE Transactions on Plasma Science, Vol. 29 (2001), no. 5, p. 722-725

[19] J. von Stebut, F. Lapostolle, M. Bucsa, H. Vallen, Surface and Coating Technology 116-119 (1999) 160-171.

[20] Y.Z. Pappas, A. Kontsos, T.H. Loutas, V. Kostopoulos, "On the characterization of continuous fibres fracture by quantifying acoustic emission and acousto-ultrasonic waveforms”, NDT&E international, to be published.